Aquaculture 594 (2025) 741457

Contents lists available at ScienceDirect

Aquaculture

journal homepage: www.elsevier.com/locate/aquaculture

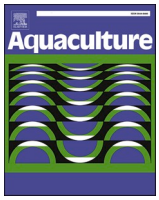

Characterization of a new peritrophin homolog from *Scylla paramamosain* and its role in molting and immune defense

Roushi Chen [a], Jiaojiao Yan [a], Shuang Li [a], Ke-Jian Wang [a,b,c], Fangyi Chen [a,b,c,*]

[a] State Key Laboratory of Marine Environmental Science, College of Ocean & Earth Sciences, Xiamen University, Xiamen 361102, Fujian, China
[b] State-Province Joint Engineering Laboratory of Marine Bioproducts and Technology, College of Ocean & Earth Sciences, Xiamen University, Xiamen 361102, Fujian, China
[c] Fujian Innovation Research Institute for Marine Biological Antimicrobial Peptide Industrial Technology, College of Ocean & Earth Sciences, Xiamen University, Xiamen 361102, Fujian, China

ARTICLE INFO

Keywords:
Molting
Bacterial infection
Peritrophin
SpPT1
Immune defense

ABSTRACT

Pathogenic infections are one of the main causes of molt failure and high mortality during molting on mud crab (*Scylla paramamosain*) farms. However, the molecular mechanisms associated with the immune defense during crab molting have not been clearly elucidated. Peritrophin, a classical chitin-binding protein, plays a key role in molting development and immunity of insects and crustaceans. In the present study, a new peritrophin homologous gene, SpPT1, was identified in *S. paramamosain*, and its full-length cDNA sequence was containing a single type II chitin-binding domain. During mud crab development, the SpPT1 gene was highly expressed at the zoea V stage, and its transcripts were significantly upregulated after molting compared to the pre-molt stage of juvenile crabs, particularly in the presence of bacterial exposure. A similar pattern was observed in the gills and subcuticular epidermis during molting in subadult crabs. Interestingly, this gene is regulated by 20E, a key steroid hormone during molting. In adult crabs, the highest expression of SpPT1 was detected in the midgut, followed by the stomach and hepatopancreas. This gene responded significantly to bacterial challenge in the hepatopancreas. Recombinant SpPT1 (rSpPT1) expressed in prokaryotes exhibited potent binding activity to chitin and several common aquatic pathogens, such as *Vibrio alginolyticus*, *Vibrio parahaemolyticus*, and *Aeromonas hydrophila*, as well as to four pathogen-associated molecular patterns (PAMPs). Notably, rSpPT1 promoted the phagocytosis of hemocytes in a dose-dependent manner *in vitro*, enhanced the clearance of *V. alginolyticus* from the hepatopancreas and gills, and significantly increased the survival of subadult *S. paramamosain* after bacterial infection *in vivo*. In addition, rSpPT1 markedly upregulated the expression of immune-related genes and enhanced the enzymatic activities of acid phosphatase and peroxidase in the hepatopancreas. Taken together, this study demonstrates that the peritrophin homolog SpPT1 might play a role in immune defense during molting, which provides new perspectives for the development of strategies to effectively control molt failure on crab farms.

1. Introduction

The mud crab *S. paramamosain* is an important mariculture species with high nutritional and economic value, and its total production in China in 2022 was 154,661 tons (Wang and Wu, 2023). Throughout its life cycle, *S. paramamosain* undergoesseveral developmental stages, including embryonic, larval, juvenile, subadult, and adult stages, during which it undergoes multiple molts (Li et al., 2022). During molting, *S. paramamosain* is more fragile and easily affected by various factors, such as sudden environmental changes, nutritional deficiencies, and pathogenic infections (particularly *Vibrio spp.* infection). These can lead to molt failure or result in a high mortality rate, accounting for 30–80% of the total mortality rate of mud crabs, which causes significant losses to the mud crab aquaculture industry (Gong et al., 2015; Yan, 2012). Currently, measures are implemented to cope with molt failure caused by sudden environmental changes and nutritional deficiencies (Yan, 2012). However, no effective strategies for preventing molt failure caused by pathogenic infections have been identified. Revealing the molecular mechanisms of immune defense during molting will help develop preventive and control measures against molt failure. Immune-

* Corresponding author at: College of Ocean & Earth Sciences, Xiamen University, Xiamen, Fujian 361102, China.
E-mail address: chenfangyi@xmu.edu.cn (F. Chen).

https://doi.org/10.1016/j.aquaculture.2024.741457
Received 5 January 2024; Received in revised form 6 June 2024; Accepted 4 August 2024
Available online 6 August 2024

related genes, such as antimicrobial peptides (AMPs), inflammatory genes, phenol oxidase activation signaling pathway, Toll signaling pathway, and antioxidant genes, were significantly upregulated in the post-molt stage of mud crabs (soft-shell crabs) (Xu et al., 2020). Interestingly, peritrophin, a typical chitin-binding protein (CBP) and peritrophic membrane (PM) protein, has been reported to play an important role not only in molting, but also in immune defense in insects (Wang et al., 2020; Zha et al., 2020).

Chitin, as a predominant component of both the *endo-* and exoskeletons in crustaceans, plays a pivotal role in both physical immune defense and molting development (Liu et al., 2019). Previous studies on arthropods, including insects and crustaceans, identified an extensive family of CBPs that possess one or more chitin-binding domains (CBDs) (Tynyakov et al., 2015), most of which belong to the type II chitin-binding domain (ChtBD2) (Tynyakov et al., 2015), such as peritrophin (Hegedus et al., 2019). cuticular proteins analogous to peritrophins (CPAPs) (Jasrapuria et al., 2010) and chitinases (Merzendorfer, 2013). In insects, these protein families have been intricately associated with immune responses and developmental processes of molting, such as the CBP SfPER from *Spodoptera frugiperda* (Rodríguez-de la Noval et al., 2019), CPAP proteins from *Tribolium castaneum* (Jasrapuria et al., 2012), peritrophin Dcy from *Drosophila melanogaster* (Kuraishi et al., 2011), and the peritrophin gene Bm01504 in *Bombyx mori* (Zha et al., 2020).

PM proteins have also received attention in crustaceans, but studies are relatively limited. PM protein is commonly referred to as a peritrophin-like protein, and it shares homology with insect peritrophins (Xie et al., 2015), and chitin-binding proteins (CBPs) (Xu et al., 2021). In shrimp, a number of peritrophin protein homologs have been identified in the acellular yolk membrane, designated as shrimp ovarian peritrophins (SOP), including SOP in *Penaeus semisulcatus* (Khayat et al., 2001), Fm-SOP from *Fenneropenaeus merguiensis* (Loongyai et al., 2007), and SOP-like protein from *Litopenaeus vannamei* (Ma et al., 2017). They exhibit chitin-binding activity and play a crucial protective role during oogenesis. The recombinant Fm-SOP also exhibited chitinase activity, effectively inhibiting the growth of *Vibrio harveyi* and *Staphylococcus aureus* (Loongyai et al., 2007). Most peritrophin-like proteins reported in shrimp areinvolved in pathogen infection and host immune response processes. Such as FcPT (Du et al., 2006), a peritrophin-like protein, identified from *Fenneropenaeus chinensis*, shares homology with insect peritrophin and SOP, containing three ChtBD2, and the recombinant FcPT had binding activity to *Escherichia coli* (Du et al., 2006). Two peritrophin-like proteins have been shown to be associated with WSSV infection, such as EcPT from *Exopalaemon carinicauda* and LvPT from L. *vannamei*. EcPT was upregulated upon WSSV challenge, and knockdown of its gene increased the survival rate of shrimp infected with WSSV, indicating its involvement in the infection process (Wang et al., 2013). LvPT interacted with a variety of viral envelope proteins (VP37, VP32, VP8A, VP39B, and VP41A), and RNAi treatment significantly reduced WSSV load and inhibited viral replication (Chen et al., 2022; Xie et al., 2015). However, few studies have been conducted on PM proteins in crabs. EsPT, a peritrophin-like protein from *Eriocheir sinensis*, is predominantly expressed in the hepatopancreas and responds significantly to various stimuli such as lipopolysaccharides and peptidoglycans, as well as infections caused by *S. aureus*, *V. parahaemolyticus*, and *Aeromonas hydrophila* (Huang et al., 2015). Furthermore, siRNA interference against EsPT impeded the elimination of *V. parahaemolyticus* (Huang et al., 2015). These findings suggest that peritrophin-like proteins play a pivotal role in the innate immunity of crustaceans. However, the role of peritrophin-like proteins during crustacean molting has not yet been elucidated and requires further in-depth study.

In this study, we screened and characterized a novel peritrophin-like gene, named SpPT1, from the transcriptome database of *S. paramamosain* established in our laboratory. The full-length cDNA sequences of SpPT1 were obtained using RACE-PCR. We analyzed the expression profiles of this gene at different developmental stages pre- and post-molt in juvenile and subadult crabs; tissue distribution in adult crabs; and the expression pattern in response to bacteria using quantitative real-time PCR (qPCR). Subsequently, the recombinant protein of SpPT1 (rSpPT1) was expressed and purified using a prokaryotic expression system and affinity chromatography, respectively. *In vitro* experiments were conducted to investigate the immune-related functions of rSpPT1, including its binding activity and phagocytosis-promoting effects. Finally, we evaluated the anti-infective effect of rSpPT1 in subadult crabs *in vivo* by calculating the survival rate and bacterial clearance capacity of crabs infected with *V. alginolyticus*, and its effect on immune-related genes and enzymatic activities. This study provides an important scientific basis for the development of treatment strategies for molt failure in mud crab aquaculture.

2. Materials and methods

2.1. Animals, strains, sample collection and immune challenge

Subadults mud crabs (50 ± 10 g), and adult mud crabs (300 ± 30 g) were purchased from the local crab farm in Zhangpu County, Fujian Province, China. Since local crab farmers only raised relatively large-sized crabs such as subadult or adult crabs, we cooperated with the Guangxi Institute of Oceanology (Guangxi Province, China) to collect samples of mud crab at various developmental stages, including the embryonic stages (E1-E5), larval stages (Z1-Z5), and megalopa stage, as well as the molting process of the juvenile crabs (pre-molt and post-molt), from a crab breeding farm in Beihai City, Guangxi Province, China, which has mature crab breeding technology. The gills and subcuticular epidermis from subadult crabs during molting periods were collected. Bacteria used in the study was purchased from China General Microbiological Culture Collection Center (CGMCC). *S. aureus* (CGMCC NO. 1.2465) and *V. alginolyticus* (CGMCC NO. 1.1833) were used to explore the role of the SpPT1 gene in the process of bacterial infection. *V. parahaemolyticus* (CGMCC NO. 1.1615), *Vibrio fluvialis* (CGMCC NO. 1.1609), *V. harveyi* (CGMCC NO. 1.1593), *Pseudomonas fluorescens* (CGMCC NO.1.3202) and *A. hydrophila* (CGMCC NO.1.2017) were used to investigated the binding activity of rSpPT1. All of the above bacteria were viable when used in subsequent experiments.

Tissues were collected from normal male and female adult mud crabs (300 ± 30 g, $n = 6$), including hemocytes (Hc), esophagus (Ep), stomach (St), foregut (Fg), midgut (Mg), hindgut (Hg), eyestalk (Es), gills (Gi), brain (Br), subcuticular epidermis (SE), hepatopancreas (Hp), heart (Ht), thoracic ganglion (TG), muscle (Mu), testis (T), anterior vas deferens (AVD), seminal vesicle (SV), posterior vas deferens (PVD), ejaculatory duct (ED), posterior ejaculatory duct (PED), ovaries (OA), and reproductive duct (RD).

The second-instar juvenile mud crabs were cultured in artificial seawater containing 7×10^6 CFU/mL of *S. aureus* and *V. alginolyticus*, respectively, with the same concentration of bacteria replaced daily. The crabs cultured in normal artificial seawater were used as the control group. The third-instar juvenile mud crabs with soft shell were collected after natural molting and stored at −80 °C for later use. 20-hydroxyecdysone (20E) dissolved in DMSO was injected at a dose of 0.2 μg/g into the base of the penultimate appendage of the juveniles (JU3). The control group was injected with the same dilution of DMSO. Samples of juveniles were collected at 3, 6, 12, 24, and 48 h after injection ($n = 4$).

To understand the immune-related function of the the SpPT1 gene, we analyzed the expression pattern of this gene in the hepatopancreas of mud crabs following injection with *V. alginolyticus* and *S. aureus*. Sixty male crabs (300 ± 30 g, $n = 5$) were temporarily cultured in the laboratory for 2 days and were randomly divided into three groups, including the control group (injection with crab saline), *V. alginolyticus*-infected group (3×10^6 CFU/crab), and *S. aureus*-infected group (3×10^6 CFU/crab). The injections were made between the third and fourth appendages of the crabs, and the hepatopancreas of five individuals were collected at 3, 6, 12, and 24 h after injection, and the samples were stored at −80 °C for subsequent qPCR analysis. All animal procedures

were carried out in strict accordance with the Animal Welfare and Ethics Committee of Xiamen University.

The extraction of total RNA from all collected samples was carried out employing Trizol reagent (Thermo Fisher Scientific, USA), while the synthesis of the corresponding cDNA was accomplished using the PrimeScript™ RT reagent kit with gDNA eraser (TaKaRa, Japan) according to the manufacturer's specified instructions.

2.2. Cloning of the full-length cDNA of SpPT1 gene

The specific primers for the SpPT1 gene (Table 1) were designed using NCBI Primer-BLAST and synthesized by Xiamen Primus Biotechnology Co., Ltd. (Xiamen, China). These primers were based on partial sequences from the transcriptome database established by our research group. For amplifying the coding sequence (CDS) of the SpPT1 gene, the cDNA extracted from the mud crab midgut served as the template, with the primers SpPT1-CDS-F and SpPT1-CDS-R. The 3′- and 5′- RACE cDNA templates of midgut tissue were prepared by the method as described previously (Qiu et al., 2021). Amplification of the 5′- untranslated region (UTR) and 3′-UTR of the SpPT1 gene was conducted using nested PCR. In the initial PCR reaction, primers SpPT1–5′-R1 and SpPT1–3′'-F1 were used, followed by the use of primers SpPT1–5′-R2 and SpPT1–3′-F2 in the second PCR reaction. Universal primers provided in the SMARTer® RACE 5′/3′ Kit were also employed. The touch-down PCR procedure consisted of the following steps: 95 °C for 5 min; 30 cycles of 95 °C for 30 s, 68 °C decreasing by 0.5 °C per cycle for 30 s, and 72 °C for 2 min; followed by 72 °C for 5 min and 16 °C for 5 min. Subsequently, the PCR products were purified and subjected to sequencing.

2.3. Bioinformatics and phylogenetic tree analysis of SpPT1 gene

Bioinformatics analysis of the SpPT1 gene was performed using several online websites. For example, the physicochemical properties analysis of protein was predicted by the Expasy ProtParam tool (https://web.expasy.org/protparam/). The SignaIP-5.0 Server (https://services.healthtech.dtu.dk/services/SignalP-5.0/) was used for signal peptide prediction. The preserve domain of protein was predicted by the SMART database (http://smart.embl-heidelberg.de/index2.cgi). The 3D structure of the protein was predicted using I-TASSER (https://zhanggroup.org/I-TASSER/). The phylogenetic tree was constructed by MEGA-X (using neighbor-joining method, 3000 bootstrap replications). Multiple sequence alignment was conducted by DNAMAN software version 8.0.

Table 1
Sequences of primers used in this study.

Primer name	Primer sequences (5′-3′)
SpPT1-CDS-F	ATGCAGCTTACCTTGATCCT
SpPT1-CDS-R	TTAGATGGTGGTGTCGTAGTC
SpPT1–5′-R1	GGTAGTGGTGATCATGTCTGCAG
SpPT1–5′-R2	TGTATCTTGTACGTGAGCCTTGG
SpPT1–3′-F1	ACCCTATCCTCATTACATGGCC
SpPT1–3′-F2	TCCTGGAATATTGCCTTCCTCA
SpPT1-qPCR-F	ACACCACCACTACTGCCATCAA
SpPT1-qPCR-R	ACCATGTCCCTCTTCAGCCTTAC
SpCrustin3-qPCR-F	ACCTGCCTGGCCATTACGTG
SpCrustin3-qPCR-R	CCCACCACAGGGAGTGTTGC
SpCrustin4-qPCR-F	CCTGCCTGGCCATTACGTGT
SpCrustin4-qPCR-R	GCTTGCACACCTTCGCTTCG
SpCrustin6-qPCR-F	ACCCTGGCAAGTGTCCCCAC
SpCrustin6-qPCR-R	TGGTGTTCAAGGCAGGCATCA
SpALF7-qPCR-F	CTTGACCCGCAGTTTTTCTGG
SpALF7-qPCR-R	TAACCACACCTTGGCTTCCT
SpIMD-qPCR-F	GGTCGTCAACATCACGGGCA
SpIMD-qPCR-R	CTCTCGCATCTGAGCAGGGC
SpTAK1-qPCR-F	GGCAGTGAAGAAGGTGGAGACAGA
SpTAK1-qPCR-R	CAGCCTTGGCACACTGGAACA
SpIKKβ-qPCR-F	CACGGCTTCTGGCTCTCCTGAT
SpIKKβ-qPCR-R	GATGGCGGGCTTGTAACTTTGCTA
SpIKKε-qPCR-F	GGTCATGCAGTCAAGCGCAAGA
SpIKKε-qPCR-R	TGCACGTGGTTCAGCTGTGA
SpRelish-qPCR-F	AGTGGAACAGTGGTCCAGCTG
SpRelish-qPCR-R	CACCACCACTTCACAAATC

2.4. Quantitative real-time PCR (qPCR) analysis

Absolute qPCR was used to analyze the tissue distribution of SpPT1 gene in *S. paramamosain*. Relative qPCR was employed to detect the expression pattern of SpPT1 gene in the hepatopancreas under bacterial challenge (*V. alginolyticus* and *S. aureus*), and the expression of SpPT1 gene in the gills and subcuticular epidermis of juvenile mud crabs during molting. qPCR was performed using a CFX384 fluorescence quantitative PCR instrument (Bio-Rad, USA), and the PCR procedure was consistent with that previously reported (Qiu et al., 2021). Finally, the relative qPCR data were analyzed using the $2^{-\triangle\triangle Ct}$ method (Livak and Schmittgen, 2001).

2.5. Expression and purification of recombinant SpPT1

For the construction of recombinant protein (rSpPT1) in the pET-30a vector (containing 6× His tag), *Nde* I and *Xho* I were chosen as the restriction enzymes based on the verified SpPT1 CDS sequence. The resulting plasmid was then transformed into the *E. coli* Transetta (DE3) strain for expression. Optimal conditions for rSpPT1 expression were established as follows: induction was carried out for 8 h at 28 °C when the OD_{600} value reached 0.4–0.5, in the presence of IPTG at a final concentration of 0.5 mM. Subsequently, the recombinant protein rSpPT1 was purified through affinity chromatography utilizing the ÄKTA Pure system (GE Healthcare Life Sciences, USA) and HisTrap™ FF Crude column (GE Healthcare Life Sciences, USA). The purified proteins underwent SDS-PAGE electrophoresis, and confirmation of the target protein bands was conducted by the Mass Spectrometry Center at the College of Life Sciences, Xiamen University. The protein concentration was quantified using the Pierce BCA Protein Assay Kit (Thermo Fisher Scientific, USA).

2.6. Binding assay

2.6.1. Chitin

The binding ability of rSpPT1 to chitin was detected using Western-blot. In a total volume of 50 μL of TBS buffer, 5 mg of chitin was incubated with 5 μg of rSpPT1 at 4 °C overnight. After incubation, the supernatant was collected by centrifugation at 12,000*g* for 3 min. The precipitate was washed three times with 200 μL TBS, and the protein was eluted with 200 μL of 7% SDS, followed by three washes with 200 μL of TBS. The supernatant after each wash was collected. Finally, the precipitate was resuspended in 200 μL of TBS. All collected samples underwent Western blot detection. The process involved transferring purified His-tagged rSpPT1 onto a PVDF membrane, which was subsequently blocked using 5% skimmed milk in Tris-buffered saline Tween-20 (10-mM Tris-HCl, 150-mM NaCl, and 0.05% *v*/v Tween-20). The membrane was then subjected to overnight incubation at 4 °C with a mouse anti-His antibody (diluted at 1:2000, Proteintech, USA). Subsequent to this primary incubation, the membrane underwent a 1-h incubation with horseradish peroxidase (HRP)-conjugated goat anti-mouse immunoglobulin G (IgG) secondary antibody (diluted at 1:5000, Invitrogen, USA). The detection of signals was achieved using Pierce™ ECL Western blotting substrate (Thermo Fisher Scientific, USA). This entire assay was independently repeated at least three times.

2.6.2. Microbial polysaccharide components

The ELISA assay was employed to assess the binding affinity of rSpPT1 to microbial surface components, specifically four pathogen-associated molecular patterns (PAMPs): lipopolysaccharide (LPS B5, Sigma, USA), lipoteichoic acid (LTA, L2515, Sigma, USA),

peptidoglycan (PGN from *B. subtilis*, Sigma, USA), and glucan (GLU, baker's yeast, Merck, Germany). To prepare the coating solution, LPS, LTA, PGN, and GLU were diluted to a working concentration of 40 μg/mL with ELISA coating solution (Solarbio, Beijing). These solutions were then added to 96-well plates and incubated at 4 °C overnight. Subsequently, the 96-well plates were blocked with 5% nonfat milk at 37 °C for 2 h. Various concentrations of the recombinant protein rSpPT1 (ranging from 0 to 4 μM) were added and incubated at 37 °C for 2 h. Following this, the primary antibody (mouse anti-His antibody, 1:3000, Proteintech, USA) was introduced and incubated at 37 °C for an additional 2 h. Subsequent to the primary antibody incubation, the secondary antibody (goat anti-mouse HRP antibody, 1:500, Invitrogen, USA) was added and incubated for another 2 h at 37 °C. The absorbance at 450 nm was measured using a microplate reader (TECAN GENios, GMI, USA). Data were recorded, and the binding efficiencies, represented by the apparent dissociation constant (Kd), were analyzed. Each group underwent three independent replicates in parallel, and the entire assay was repeated at least three times.

2.6.3. Aquatic pathogens

The binding ability of rSpPT1 to six common aquatic pathogens (including *V. alginolyticus*, *V. parahaemolyticus*, *V. fluvialis*, *V. harveyi*, *A. hydrophila*, and *P. fluorescens*) was analyzed using Western blot. The above bacteria were adjusted to a working concentration ($OD_{600} = 1$) with TBS. 200 μL of bacterial solution was incubated with 200 μL rSpPT1 (final protein concentration of 40 μg/mL), and incubated at room temperature for 1 h (rSpPT1 did not appear to be visibly digested after incubation with these live bacteria). After incubation, the samples were centrifuged at 6000*g* for 5 min and the supernatants were collected. The bacterial precipitate was washed 3 times with 400 μL TBS and eluted with 400 μL 7% SDS. The eluted supernatant was collected. After that, the bacteria were washed twice with 400 μL TBS, and finally the bacteria were resuspended and precipitated with 400 μL TBS. All the samples obtained were subjected to SDS-PAGE electrophoresis followed by Western blot analysis. The independent assay was repeated at least twice.

2.7. Phagocytosis assay

Mud crab hemocytes were isolated as previously reported (Jiang et al., 2022) and adjusted to 1×10^6 per tube with L-15 medium containing 5% FBS and 1.2% NaCl. Different concentrations of rSpPT1 (25 mg/mL, 50 mg/mL, 100 mg/mL) were added and incubated for 30 min. An equal volume of L-15 medium was used as control. After that, 1×10^7 fluorescent microspheres (1:10 ratio to hemocytes) were added and incubated for 45 min. After incubation, the hemocytes were fixed with 2% glutaraldehyde solution for 15 min. The nuclei of the hemocytes were stained with DAPI (Beyotime, China), and fluorescence microsphere was detected by FITC channel. Phagocytosis of fluorescent microspheres by hemocytes was observed using a laser confocal microscope (CLSM, Zeiss Lsm 780 NLO, Germany). The phagocytosis efficiency of hemocytes was determined by flow cytometry (CytoFLEX, Beckman Coulter, USA). The independent assay was repeated three times.

2.8. Effects of rSpPT1 on S. paramamosain infected with V. alginolyticus

2.8.1. Cytotoxicity assay

The hemocytes extracted from adult crabs were primarily cultured (Kun et al., 2014) and the effect of rSpPT1 on hemocyte cytotoxicity was assessed using the MTS method (Yang et al., 2020). In brief, approximately 1×10^5 cells/well were seeded in 96-well cell culture plates at 28 °C and allowed to incubate for 6 h. Various concentrations of rSpPT1 (1.5, 3, 6, 12, and 24 μM) were then introduced and incubated for an additional 24 h. The CellTiter 96® AQueous Kit (Promega) was utilized to gauge hemocyte viability. Each concentration of rSpPT1 treatment was conducted with three biological replicates. The independent experiment was repeated at least three times.

2.8.2. Hemolytic activity assay

The hemolytic activity of rSpPT1 on mouse erythrocytes was evaluated following established procedures (Zhu et al., 2021). Fresh mouse erythrocytes were thoroughly washed and adjusted to a concentration of 5×10^9 cells/mL with 0.9% NaCl. Subsequently, various concentrations of rSpPT1 (1.5, 3, 6, 12, and 24 μM) were added and incubated at 37 °C for 1 h. Negative control and positive control treatments included PBS and 0.5% Triton X-100, respectively. The absorbance at 540 nm was recorded using a microplate reader, and hemolysis rates were calculated based on previously established methods. (Zhu et al., 2021).

2.8.3. Mortality test

To assess the potential anti-infective effect of rSpPT1 *in vivo*, bacterial challenge experiment was conducted on male subadult mud crabs (80 ± 10 g), which have been shown to be more susceptible to *V. alginolyticus* infection. All crabs were injected with *V. alginolyticus* (1×10^6 CFU/crab) at the base of the right fourth leg ($n = 50$). After 1 h of injection, the crabs were divided into two groups of 25 crabs each. The control group received a 40 μL injection of PBS, while the experimental group was injected with 40 μL of rSpPT1 (5 μg/crab), which was diluted by PBS. The survival of crabs was recorded at various time points, and mortality curves were generated using GraphPad Prism (version 8.3.0). The independent experiment was repeated twice.

2.8.4. Bacterial load assay

The bacterial loads of *V. alginolyticus* in the hepatopancreas and gills of crabs from the PBS and rSpPT1 injection groups (5 μg/crab) were counted at 3, 6, 12 and 24 h after treatment. Hepatopancreas and gills ($n = 5$) were collected at each time point by adding 1 mL of PBS per 500 mg of tissue sample. They were then homogenized and the homogenates were diluted to the appropriate multiplicity and then plated onto 2216E agar plates (Qingdao Hope Bio Tech., China), and incubated at 28 °C overnight. Bacterial CFUs were counted and recorded for all plates.

2.8.5. Enzymatic activity assay and immune-related genes expression analysis

One hour after *V. alginolyticus* (1×10^6 CFU/crab) challenge, crabs were treated with rSpPT1 (5 μg/crab), and the hepatopancreas ($n = 3$) were collected at 3, 6, 12, and 24 h after treatment. For enzyme activity assay, the hepatopancreas were homogenized as described above, and the enzyme activities of the samples were detected using the corresponding enzyme activity assay kits, including acid phosphatase (ACP) and peroxidase (POD) (Nanjing Jiancheng, China). For immune-related genes expression analysis, qPCR was used to detect the changes in genes expression in hepatopancreas, including antimicrobial peptide genes (SpCrustin3, SpCrustin6, SpALF7) and immune-related signaling pathway genes (SpIMD, SpTAK1, SpIKKβ, SpIKKε, SpRelish). The primers of the above genes were shown in Table 1.

2.9. Statistical analysis

The statistical analyses were conducted using GraphPad Prism version 8.3.0. In the case of relative qPCR analysis, enzymatic activity analysis, and bacterial load analysis, unpaired *t*-tests were employed. Mortality curves were generated using GraphPad Prism and subjected to analysis using the Kaplan-Meier Log rank test. Statistical significance was considered at $p < 0.05$. All data were presented as mean ± standard deviation (SD).

3. Results

3.1. Sequence and structural analysis of SpPT1

The full-length cDNA sequence of the SpPT1 gene (GenBank Accession NO. OQ886067) was 796 bp, including a 5′ untranslated region (UTR) of 51 bp, a 3′ UTR of 326 bp, and an open reading frame (ORF) of 402 bp (Fig. 1A). The ORF of the SpPT1 gene encoded a total of 133 amino acids (aa), of which 1–22 aa were signal peptides. The mature SpPT1 peptide had a total of 111 aa, with a molecular weight of 11.9 kDa, and a pI of 4.50. SpPT1 has a chitin-binding domain, ChtBD2 (Fig. 1B), which has six conserved cysteines and belongs to the peritrophin-A type. The 3D structural prediction of the SpPT1 protein showed that it had four β-sheets and three α-helical structures (Fig. 1C).

Phylogenetic tree analysis showed that the SpPT1 gene was located in the same branch with MnPT from *Macrobrachium nipponense*, EsPT from *E. sinensis* and PcPT from *Palaemon carinicauda* (Fig. 1D). In addition, the amino acid sequence identity between SpPT1 and the other peritrophin-like genes were 26.42%–35.14%, with the highest rate (35.14%) between SpPT1 and PcPT (Table 2).

3.2. SpPT1 gene expression profiles

Distribution of the SpPT1 gene at different developmental stages (embryo I-V, zoea I-V, megalopa, juvenile I), molting stages of juvenile and subadult crabs, in different tissues of adult crabs, as well as gene expression patterns in response to bacterial and 20E challenges were investigated. The results showed that the SpPT1 gene reached the highest expression level of 6×10^5 copies/μL at the zoea V (Z5) stage (Fig. 2A). The expression of this gene was significantly upregulated in the post-molt stage of juvenile crabs compared to that in the pre-molt stage (Fig. 2B), as well as in the gills and subcuticular epidermis of

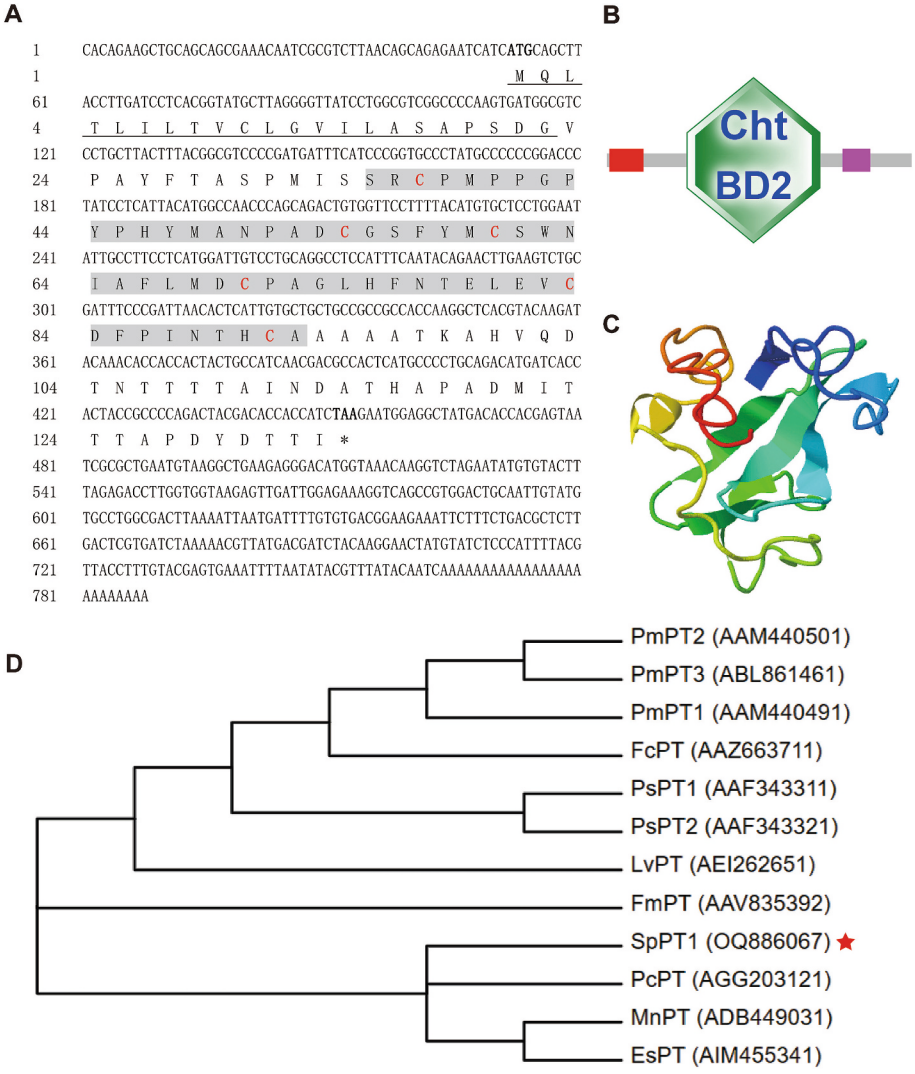

Fig. 1. Bioinformatics and phylogenetic analysis of SpPT1. (A) The nucleotide sequence and deduced amino sequence of SpPT1 from *S. paramamosain*. Start codon (ATG) and stop codon (TAA) are marked in bold. The signal peptide is underlined and the ChtBD2 domain is highlighted in gray. Six conserved residues are marked in red. (B) Schematic representation of the structural domain of SpPT1 protein predicted by SMART. (C) A predicted three-dimensional model of SpPT1 by I-TASSER program. (D) Phylogenetic tree analysis of SpPT1. A neighbor-joining phylogenetic tree of peritrophin was constructed using MEGA-X software with 3000 bootstrap replications. SpPT1 is marked with a red pentagram. The information of the sequences is listed as follows: Pm: *Penaeus monodon*; Fc: *P. chinensis*; Ps: *Penaeus semisulcatus*; Lv: *L. vannamei*; Fm: *F. merguiensis*; Pc: *Palaemon carinicauda*; Sp: *Scylla paramamosain*; Mn: *Macrobrachium nipponense*; Es: *E. sinensis*. SpPT1 (GenBank: OQ886067), MnPT (GenBank: ADB44903.1), EsPT (GenBank: AIM45534.1), PcPT (GenBank: AGG20312.1), LvPT (GenBank: AEI26265.1), FcPT (GenBank: AAZ66371.1), PmPT1 (GenBank: AAM44049.1), PmPT2 (GenBank: AAM44050.1), PmPT3 (GenBank: ABL86146.1), FmPT (GenBank: AAV83539.2), PsPT1 (GenBank: AAF34331.1), PsPT2 (GenBank: AAF34332.1). (For interpretation of the references to colour in this figure legend, the reader is referred to the web version of this article.)

Table 2
Amino acid sequence identity of peritrophin-like genes with SpPT1 in *S. paramamosain*.

Species name	Gene name	GenBank	Identity
Scylla paramamosain	SpPT1	OQ886067	–
Macrobrachium nipponense	MnPT	ADB44903.1	30.30%
Eriocheir sinensis	EsPT	AIM45534.1	30.77%
Palaemon carinicauda	PcPT	AGG20312.1	35.14%
Penaeus vannamei	LvPT	AEI26265.1	33.96%
Penaeus chinensis	FcPT	AAZ66371.1	28.30%
Penaeus monodon	PmPT1	AAM44049.1	26.42%
	PmPT2	AAM44050.1	26.42%
	PmPT3	ABL86146.1	26.42%
Fenneropenaeus merguiensis	FmPT	AAV83539.2	32.69%
Penaeus semisulcatus	PsPT1	AAF34331.1	30.19%
	PsPT2	AAF34332.1	30.19%

subadult crabs (Fig. 2C&2D). In particular, in the presence of *S. aureus* and *V. alginolyticus*, the expression of SpPT1 after molting was higher than that in the control group (Fig. 2E). In addition, the expression was downregulated 12 h after 20E challenge (Fig. 2F).

In the tissues of adult crabs, the highest expression of SpPT1 was found in the midgut of female and male crabs, with an average of 7.4×10^7 copies/μL and 8.9×10^7 copies/μL, respectively, followed by the hepatopancreas and stomach, with approximately 1×10^5–1×10^6 copies/μL (Fig. 3A&B). Studies in insects have reported the expression of peritrophin in different segments of the digestive tract, with predominant expression in the midgut (Sandoval-Mojica and Scharf, 2016; Tellam et al., 2003; Zha et al., 2020). Notably a similar distribution pattern of this gene was observed in crabs. The digestive tract of the crabs includes the esophagus, stomach, foregut, midgut, and hindgut (Fig. 3C). The qPCR results showed that the expression of SpPT1 in the digestive tract was highest in the midgut, followed by that in the stomach, foregut, and hindgut, with the lowest expression in the esophagus (Fig. 3D). In the hepatopancreas of crabs, the expression of SpPT1 was significantly upregulated at 3, 6, 24, and 48 h after *S. aureus* challenge (Fig. 3E) and at 6 h after *V. alginolyticus* challenge (Fig. 3F).

3.3. Expression and purification of SpPT1 recombinant protein (rSpPT1)

Soluble recombinant protein rSpPT1 was successfully obtained from the prokaryotic expression system. SDS-PAGE analysis showed a specific positive band at a position near 15 kDa and a relatively high purity of rSpPT1 (Fig. 4A), which was confirmed by the mass spectrometry.

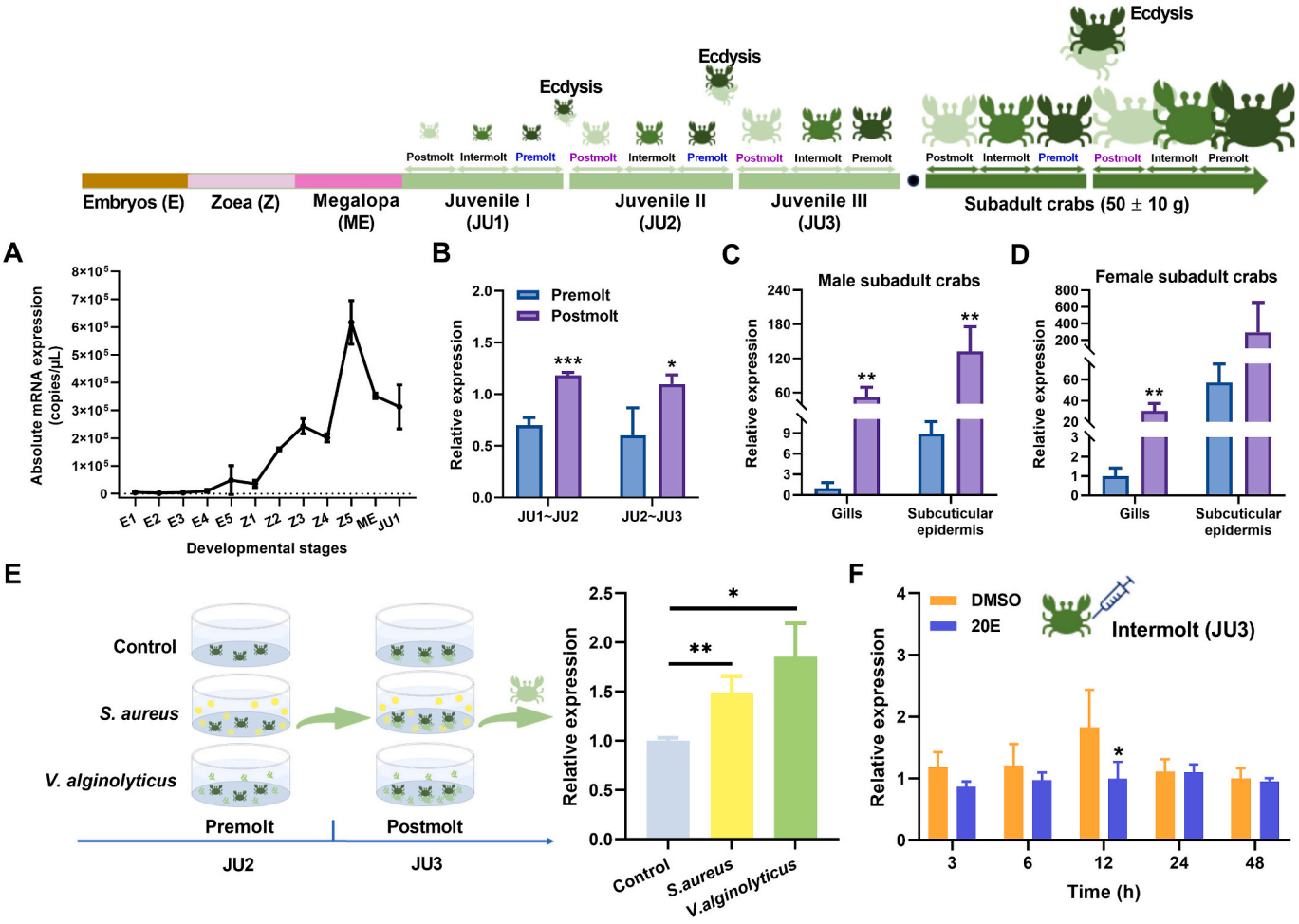

Fig. 2. Expression profiles of SpPT1 gene in the developmental stages of *S. paramamosain*. (A) The expression of SpPT1 in the different developmental stages of *S. paramamosain* was determined by absolute qPCR ($n = 3$). Em1-Em5: embryonic stage 1–5; Z1-Z5: zoeal larval stage 1–5; ME: megalopa larval stage; JU: juveniles. (B) The expression of SpPT1 in molting process of juvenile crabs was analyzed by relative qPCR (n = 3). The expression pattern of SpPT1 in gills and subcuticular epidermis during molting process of male (C) and female (D) subadult crabs was analyzed by relative qPCR (n = 3). (E) The expression pattern of SpPT1 gene in the post-molt stage of juvenile crabs in the presence of *S. aureus* and *V. alginolyticus* (n = 3). (F) The expression pattern of SpPT1 in the intermolt stage of juvenile mud crabs (JU3) after 20E stimulation ($n = 4$). Significant difference was indicated with asterisks, $^*p < 0.05$, $^{**}p < 0.01$, $^{***}p < 0.001$.

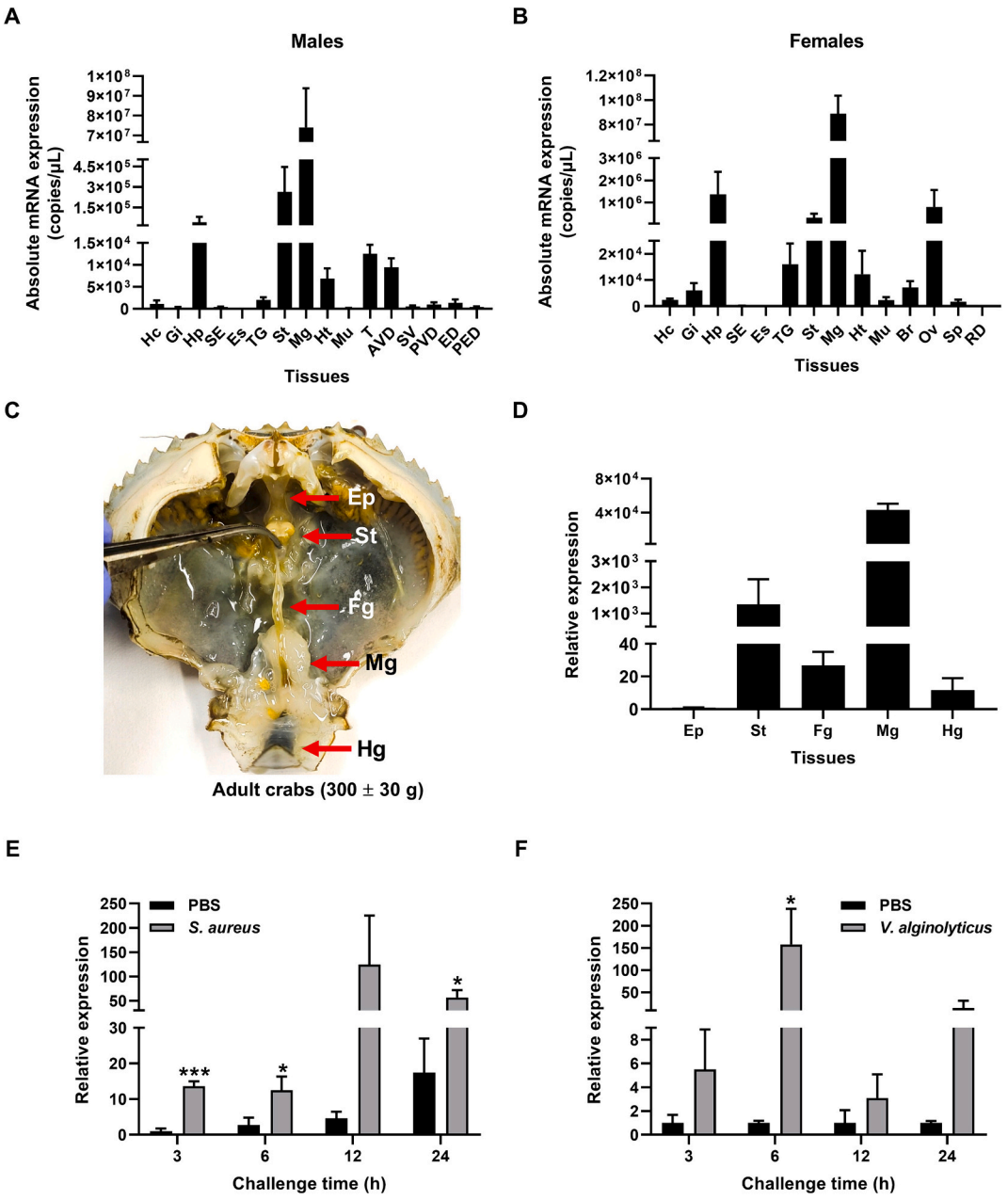

Fig. 3. Expression profiles of SpPT1 gene in adult *S. paramamosain*. Tissue distribution of SpPT1 in male (A) and female (B) crabs ($n = 5$). (C) Differentiation of various tissues of digestive tract in *S. paramamosain*. (D) Expression pattern of SpPT1 in different digestive tract tissues. The expression pattern of SpPT1 in male hepatopancreas after *S. aureus* (E) and *V. alginolyticus* (F) challenges (n = 3). Significant difference was indicated by asterisks as $^{*}p < 0.05$, $^{***}p < 0.001$. Hc, hemocytes; Gi, gills; Hp, hepatopancreas; SE, subcuticular; Es, eye stalk; TG, thoracic ganglion; Ep, esophagus; St, stomach; Fg, foregut; Mg, midgut; Hg, hindgut; Ht, heart; Mu, muscle; T, testis; AVD, anterior vas deferens; SV, seminal vesicle; PVD, posterior vas deferens; ED, ejaculatory duct; PED, posterior ejaculatory duct; Br, brain; OA, ovaries; RD, reproductive duct.

3.4. Binding activity of rSpPT1

ELISA was used to detect the binding of rSpPT1 to PAMPs (LPS, LTA, PGN, and GLU). As shown in Fig. 4B, the Kd values of rSpPT1 with the four PAMPs, LPS, LTA, PGN and GLU, were 1.195, 0.960, 0.541and 0.482 μM, respectively, meaning moderate binding ability. Western blotting results showed that rSpPT1 had a strong binding affinity for chitin, with only a small amount of recombinant protein eluted from chitin by 7% SDS (Fig. 4C). In addition, rSpPT1 exhibited significant binding ability to several common aquatic pathogens, including *V. alginolyticus*, *V. fluvialis*, *V. parahaemolyticus*, *V. harveyi*, *A. hydrophila*, and *P. fluorescens* (Fig. 4D).

3.5. Opsonization of rSpPT1

The effect of different concentrations of rSpPT1 on the phagocytosis of hemocytes *in vitro* was examined using flow cytometry and fluorescence confocal microscopy. The results showed that after treatment with 25 μg/mL (2 μM), 50 μg/mL (4 μM), and 100 μg/mL (8 μM) of rSpPT1, the hemocytes appeared to form nodules, and more green fluorescent signals were observed in the cells (Fig. 5A). The phagocytic rate of hemocytes in the control group was 23.5%, whereas that in the rSpPT1-treated group were 47.6%, 60.9%, and 63.1%, respectively, in a dose-dependent manner (Fig. 5B).

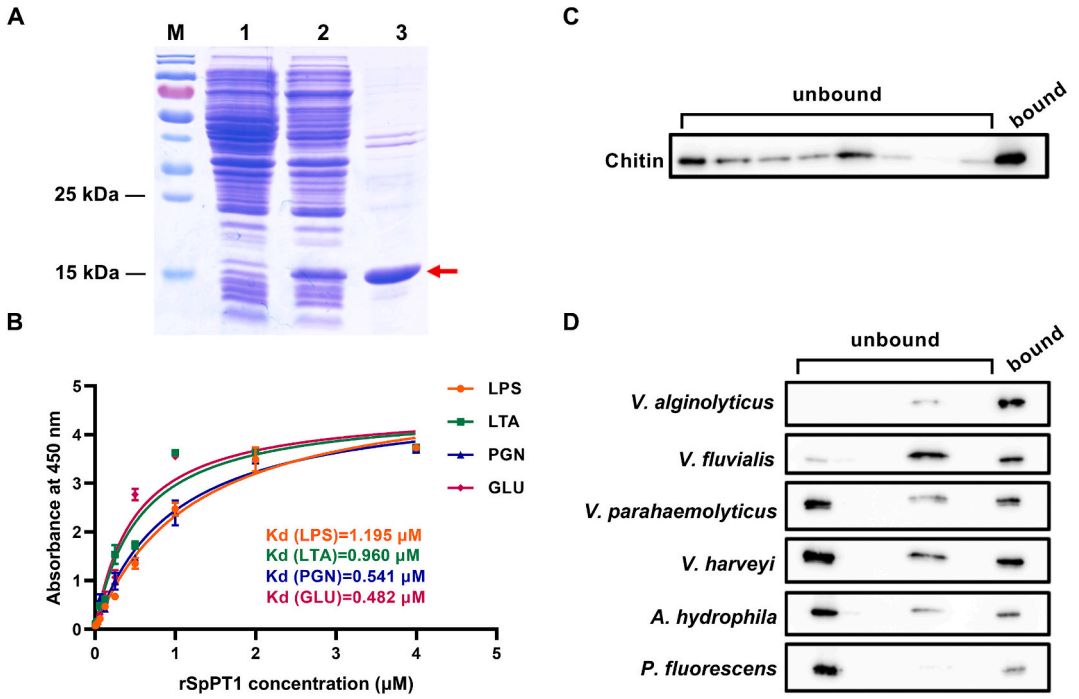

Fig. 4. Recombinant SpPT1 expression and binding activity. (A) Expression and purification of recombinant SpPT1. Lane M: protein molecular standard; lane 1: *E. coli* BL21 (DE3) containing recombinant vector (pET-30a-SpPT1) before induction; lane 2: *E. coli* BL21 (DE3) containing recombinant vector (pET-30a-SpPT1) after induction by 0.5 mM isopropyl-β-D-thiogalactopyranoside (IPTG); lane 3: purified rSpPT1. (B) Binding activity of rSpPT1 to PAMPs (LTA, lipoteichoic acid; LPS, lipopolysaccharide; PGN, peptidoglycan; GLU, Glucan). (C) Binding activity of rSpPT1 to chitin. (D) Binding activity of rSpPT1 to bacteria. The unbound lanes included the supernatant after incubation, and TBS & 7% SDS eluent. The bound lanes represented rSpPT1 that bound bacteria after washing.

3.6. Bacterial clearance and anti-infective effect

rSpPT1 showed no cytotoxic effect on crab hemocytes and no evidence of hemolytic activity on mouse erythrocytes at a concentration of 24 μM (Fig. 6A & 6B). To explore whether rSpPT1 had an immunoprotective effect on *S. paramamosain*, crabs were challenged with *V. alginolyticus* and treated with rSpPT1 as shown in Fig. 6C. The results showed that at 24 h after treatment, the survival rate of the PBS group was only 41.7%, whereas it was approximately 79.2% in the rSpPT1-treated group. After 168 h of treatment, the survival rate of the control group was only 12.5%, whereas that of the rSpPT1-treated group was 62.5% (Fig. 6C). These results indicated that rSpPT1 treatment significantly enhanced *in vivo* resistance to bacterial infection in crabs.

Bacterial loads in the gills and hepatopancreas of *S. paramamosain* were determined after bacterial infection and after different treatments. The results showed that the bacterial loads in the hepatopancreas were significantly reduced at 3, 12, and 24 h after treatment with rSpPT1 (Fig. 6D), with an average bacterial load of 6.0×10^2 CFU/g compared with 3.0×10^3 CFU/g in the control group. In the gills, similar reductions in bacterial load were observed at 3, 6, 12, and 24 h after rSpPT1 treatment (Fig. 6E), with 1.0×10^4 CFU/g in the control group and 4.0×10^3 CFU/g in the rSpPT1-treated group.

3.7. Regulation of S. paramamosain infected with V. alginolyticus by rSpPT1

To further explore the molecular mechanism of the immunomodulatory effects of rSpPT1 on mud crab, the activities of several immune-related enzymes and the expression of immune-related genes were analyzed. The results showed that the enzymatic activities of ACP (Fig. 6F) and POD (Fig. 6G) were significantly enhanced in the hepatopancreas 3 h and 24 h after rSpPT1 treatment, respectively, compared with the control group. Furthermore, IMD signaling pathway genes, including SpIMD, SpTAK1, SpIKKε, SpIKKβ and SpRelish, were significantly upregulated in rSpPT1-treated crabs, and similar expression patterns were observed for several AMPs (SpCrustin3, SpCrustin6 and SpALF7) (Fig. 7).

4. Discussion

Although the discovery of PM and peritrophins in insects has attracted significant attention (Konno and Mitsuhashi, 2019; Richards and Richards, 1977; Wang and Granados, 2001), and their importance in insect intestinal immunity has been confirmed (Eisemann and Binnington, 1994; Wu et al., 2016), studies on PM and peritrophins in crustaceans are limited. In recent years, PM (Han et al., 2019; Thuong et al., 2016) and peritrophin-like proteins homologous to insect peritrophin (Du et al., 2006; Huang et al., 2015; Loongyai et al., 2007) have been identified in crustaceans and shown to be associated with ovarian development and immunity. However, their role in the molting stages of crustaceans remains unclear.

In this study, a peritrophin-like gene, SpPT1, screened from the transcriptome database of *S. paramamosain* we established previously (Li et al., 2023), attracted our attention; its transcript level was low in the pre-molt stage, whereas it was significantly higher in the post-molt stage of juvenile crabs. First, the accuracy of the transcriptomic data was verified using qPCR. The results showed that the expression of SpPT1 was significantly upregulated in the post-molt stage of crabs, not only in juveniles, but also in the tissues of subadults, which was similar to the expression pattern of many immune-related genes (Xu et al., 2020). In addition, this gene is regulated by 20E (a steroid hormone), a key regulator of molting, suggesting that SpPT1 might be involved in the molting process. Interestingly, when juvenile crabs were challenged with *V. alginolyticus* and *S. aureus*, the representative bacterial pathogens used in the study of crustacean immunity (Chen and Wang, 2019; Dong et al., 2017), during their development to the post-molt stage, the transcript levels of SpPT1 in the exposed groups were significantly higher than those in the control group. Based on these findings, we

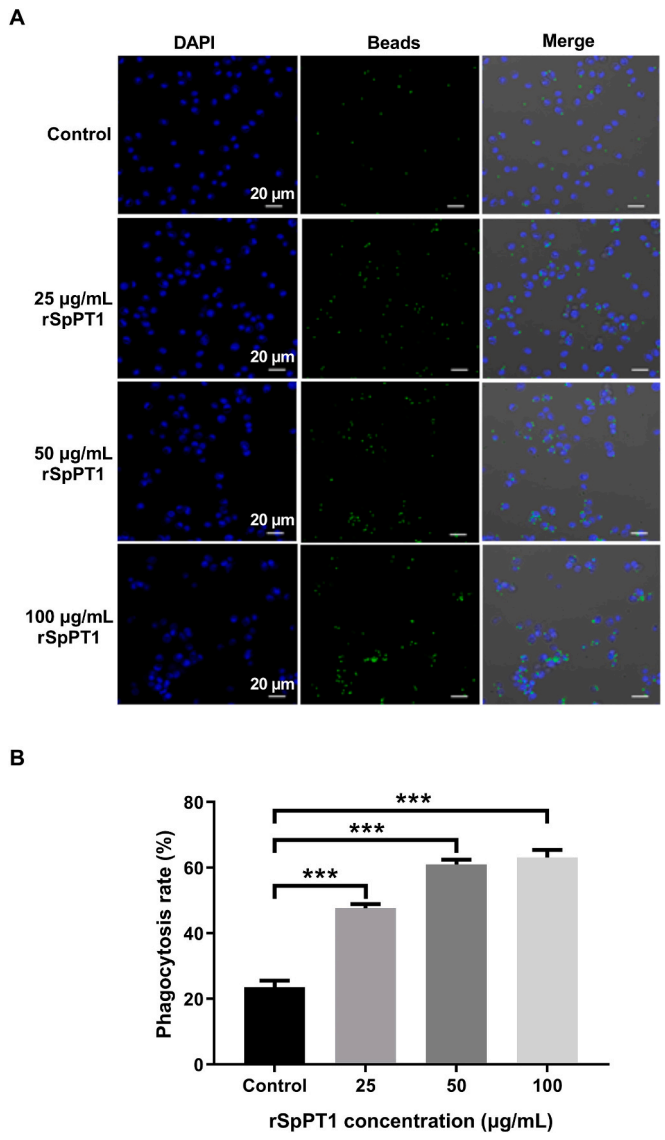

Fig. 5. Phagocytosis of fluorescent microspheres by hemocytes after rSpPT1 treatment. (A) Phagocytosis of fluorescent microspheres by hemocytes after rSpPT1 treatment (25 μg/mL, 50 μg/mL or 100 μg/mL) was observed under CLSM, and equal volume of L-15 medium was used as control. The nuclei of hemocytes were stained with 4,6-diamino-2-phenyl-indole (DAPI) (blue), and green fluorescence represented fluorescent microspheres. (B) The phagocytosis rate of fluorescent microspheres by hemocytes was determined by flow cytometry. Significant difference was indicated with asterisks, $***p < 0.001$. (For interpretation of the references to colour in this figure legend, the reader is referred to the web version of this article.)

speculate that SpPT1 may play an important role in the innate immune defense of mud crab, particularly during molting. Subsequently, we successfully obtained the full-length cDNA sequences of SpPT1 and extensively analyzed its expression profiles. Furthermore, the recombinant protein rSpPT1 was obtained, and its immune-related functions of rSpPT1 both *in vitro* and *in vivo* were investigated.

Peritrophin is an important constitutive protein that strongly binds to the chitin skeleton of the PM. It requires strong denaturants such as guanidine hydrochloride, urea, and sodium dodecyl sulfate (SDS) for elution and is classified as a class III peritrophic membrane protein (Tellam et al., 1999). Peritrophins are typically characterized by one or more cysteine-rich chitin-binding domains (ChtBD2). In insects, three different types of ChtBD2 are present and they are classified based on the number of cysteines: including peritrophin-A, peritrophin-B and peritrophin-C (Tynyakov et al., 2015), whereas only Peritrophin-A has been reported in crustaceans. Different amounts of ChtBD2 determine the complexity of the protein structure and its affinity for chitin, thereby conferring functional diversity to peritrophic proteins (Tellam et al., 1999).

In insects, peritrophins are highly expressed in the midgut and the cardia (Peters, 2012). For example, the expression levels of peritrophin-57 and peritrophin-37 in *Prodenia litura* (Chen et al., 2014) and Bm01504 in *B. mori* (Zha et al., 2020), are high in the midgut. Notably, peritrophin-95 was predominantly present in the larvae of *Pseudomonas aeruginosa* (Tellam et al., 2000), whereas peritrophin-48 was detected mainly in the cardinal valve region of *Chrysomya bezziana* larvae (Vuocolo et al., 2001). In crustaceans, FcPT (Du et al., 2006) is predominantly expressed in the intestinal and ovarian tissues of *Fenneropenaeus chinensis*, LvPT (Xie et al., 2015) is mainly distributed in the gastric tissue, and EsPT (Huang et al., 2015) is highly expressed in the hepatopancreas, intestine, and hemocytes. Studies have shown that insect PM plays a crucial role in maintaining gut health and intestinal immune defense. As a protective barrier between food and intestinal epithelial cells in the midgut, the PM serves a variety of essential physiological functions, such as protecting intestinal cells against mechanical damage (Wang and Granados, 1997), enhancing digestive efficiency (Espinoza-Fuentes and Terra, 1987), selectively allowing nutrient absorption, defending against invasion by pathogenic microorganisms (Barbehenn and Martin, 1992; Peters, 2012), and facilitating the absorption and metabolism of toxic chemicals (*e.g.*, DDT) (Abedi and Brown, 1961) and metal ions (Devenport et al., 2006). Peritrophins, which are integral proteins in the PM, contribute significantly to its physiological function. In our study, SpPT1 had a signal peptide and one ChtBD2 that were expressed predominantly in the midgut of adult crabs, suggesting that it might exert an insect-like intestinal immune function, which needs to be confirmed by further evidence.

Previous studies on crustaceans have shown that peritrophin-like proteins directly inhibit bacterial growth and are involved in immune responses. For example, the ovarian peritrophin Fm-SOP from *F. merguiensis* exhibits antibacterial activity against *V. harveyi* and *S. aureus* (Loongyai et al., 2007). However, some peritrophins are responsive to bacterial or viral infections without any antimicrobial activity, such as FcPT from *F. chinensis* (Du et al., 2006), which was significantly upregulated in hemocytes, heart, stomach, intestines, and gills in response to *S. aureus* and *Vibrio anguillarum* challenges, and EsPT from *E. sinensis* (Huang et al., 2015), which was remarkably upregulated in the hepatopancreas after stimulation by LPS or PGN, or infections with *S. aureus* and *V. parahaemolyticus*. Similarly, we found that SpPT1 responded significantly to bacterial infections in both juvenile molting stages and adults but had no direct antibacterial effect. To explore whether this protein has an immune-related function, we obtained the recombinant target protein rSpPT1 using a prokaryotic expression system and explored its *in vitro* activity and *in vivo* anti-infective effects.

Most peritrophins in insects or crustaceans have the ability to bind chitin *via* ChitBD2, such as rSOP-Sf9 and rSOP-Ec (Loongyai et al., 2007). We found that rSpPT1 also possesses strong chitin-binding activity, suggesting that it may act as a structural protein that binds to the chitinous skeleton of mud crabs, thereby participating in physiological functions (*e.g.*, recognizing pathogens, binding to toxins, and acting as an immune barrier). In addition, rSpPT1 had moderate binding affinity towards four PAMPs, with dissociation constants ranging from 0.48 to 1.2 μM, and a particularly, strong binding ability to a variety of aquatic pathogens, including *V. alginolyticus*, *V. fluvialis, V. parahaemolyticus*, *V. harveyi*, *A. hydrophila*, and *P. fluorescens*. These findings suggest that SpPT1 may possess a function analogous to that of pattern recognition receptors (PRRs) that recognize and bind PAMPs and serve as a crucial trigger for the activation of cellular and humoral immune responses (Lu et al., 2020).

We further explored whether SpPT1 played a role in the cellular immunity of mud crabs. The class B scavenger receptor (SpSR-B) (Zhou

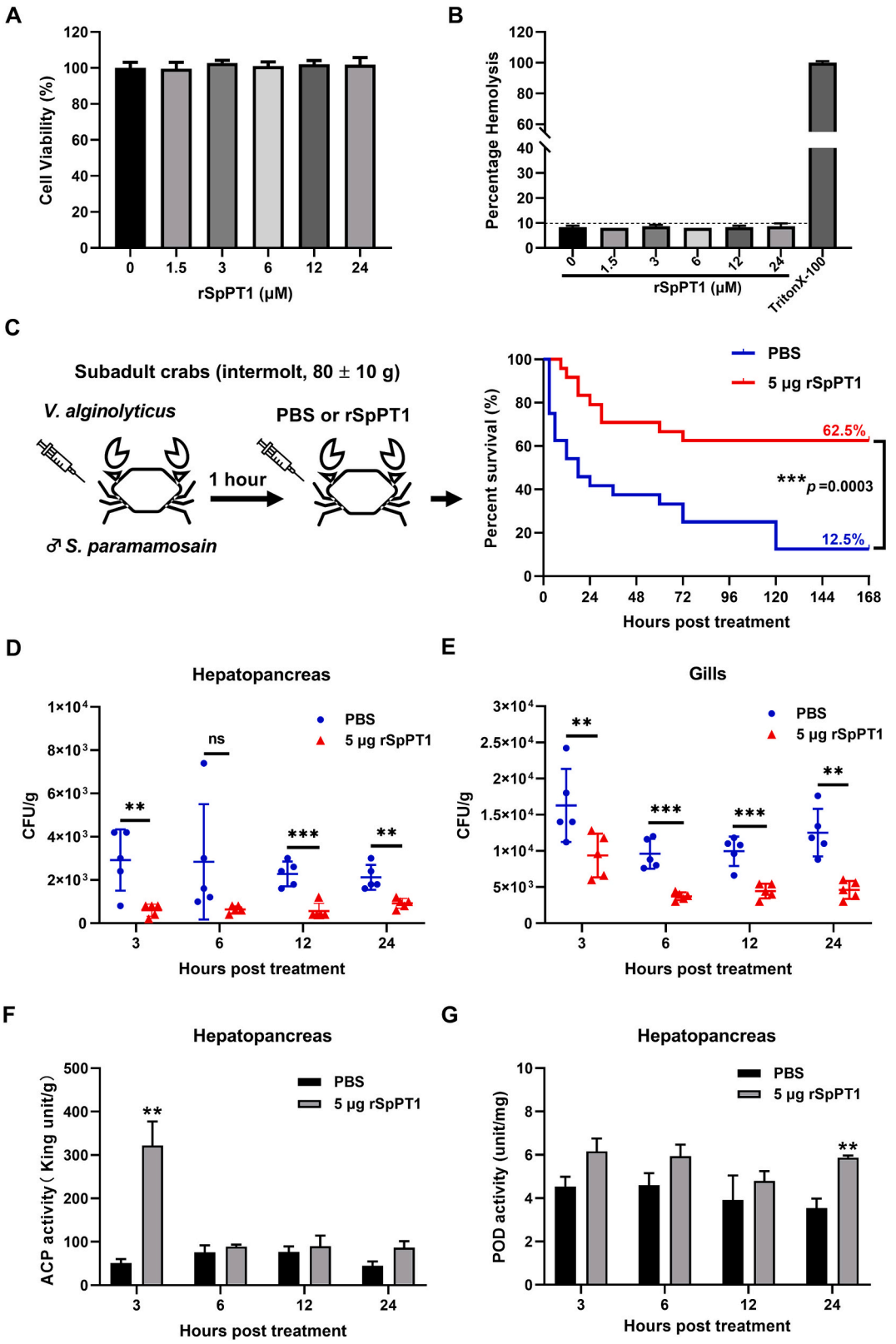

Fig. 6. The anti-infective effect of rSpPT1 in *S. paramamosain*. Cytotoxic effect of rSpPT1 on crab hemocytes (A) and hemolytic activity of red blood cells in mice (B). (C) Male subadult crabs were challenged with *V. alginolyticus*, and rSpPT1 was injected (5 μg/crab) at 1 h post bacterial challenge ($n = 25$). The survival curve of mud crabs after rSpPT1 treatment was plotted. Bacterial clearance of *V. alginolyticus* in the hepatopancreas (D) and gills (E). The bacterial load in the gills and hepatopancreas were determined at 3, 6, 12 and 24 h after rSpPT1 treatment. Enzymatic activity analysis about ACP (F) and POD (G) was measured in the hepatopancreas at 3, 6, 12 and 24 h after rSpPT1 treatment (n = 3). Significant difference was indicated with asterisks, ** $p < 0.01$ and *** $p < 0.001$. (For interpretation of the references to colour in this figure legend, the reader is referred to the web version of this article.)

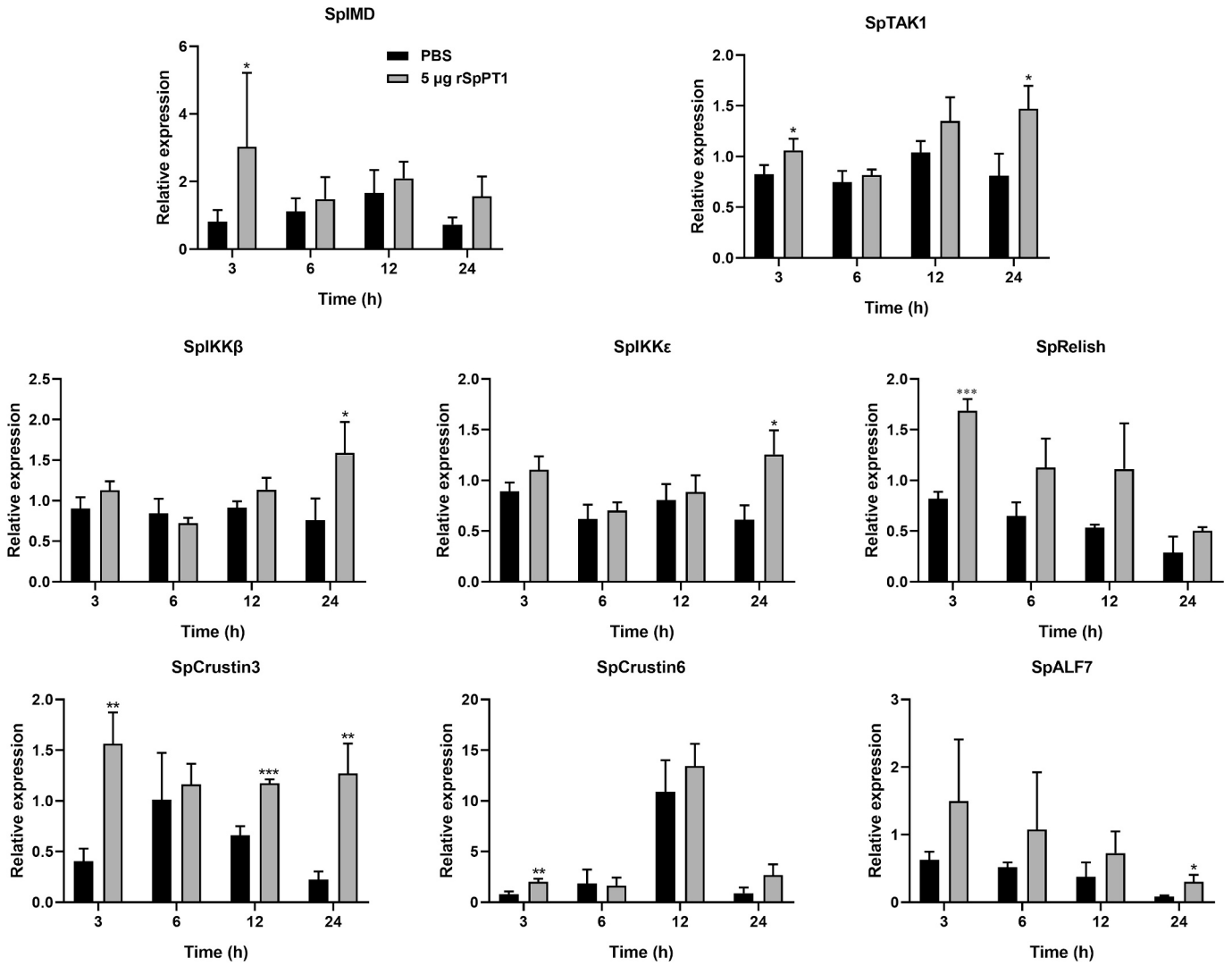

Fig. 7. The effect of rSpPT1 in *S. paramamosain*. The immune-related genes (SpIMD, SpTAK1, SpIKKβ, SpIKKε, SpRelish, SpCrustin3, SpCrustin6 and SpALF7) expression in the hepatopancreas were examined (n = 3). Significant difference was indicated with asterisks, * $p < 0.05$, ** $p < 0.01$, *** $p < 0.001$.

et al., 2021), which binds to a wide range of gram-negative and gram-positive bacteria and the promotes phagocytosis of *V. parahaemolyticus* and *S. aureus* by hemocytes, has been reported to play an important role in the cellular immunity of mud crabs. In addition to classical PRRs, some AMPs have been shown to have phagocytosis-promoting functions in hemocytes, such as SpCrus8 (Jiang et al., 2022), a member of the crustin family, which is the most classical family of AMPs in crustaceans. In *Marsupenaeus japonicus*, MjCruI-1 itself did not have antibacterial activity; however, when MjCruI-1 was injected into shrimp after co-incubation with *S. aureus* or *Vibrio europaeus*, the hemocyte phagocytosis efficiency of the experimental group was significantly higher than that of the control group. These findings provided valuable insights and prompted us to investigate whether rSpPT1 has a similar function in mud crabs. Our results confirmed that rSpPT1 indeed significantly increased the phagocytosis of fluorescent microspheres by hemocytes, leading to a remarkable increase in phagocytic activity of 39.6% at a protein concentration of 100 μg/mL. This suggests that SpPT1 might plays a role in the cellular immunity of mud crabs by acting as an opsonin that enhances the clearance of exogenous substances.

To investigate the potential role of SpPT1 in bacterial infection resistance *in vivo*, we established a bacterial infection model in mud crabs. Subadult crabs at intermolt stage were injected with *V. alginolyticus* for 1 h, followed by 5 μg rSpPT1. The results showed a significant reduction in bacterial load in the hepatopancreas and gills of the rSpPT1-treated group, which may be attributed to the opsonization effect of the protein. After 168 h of treatment, the survival rate of the mud crabs in the treated group was 50% higher than that in the control group (62.5% in the rSpPT1 treated group and 12.5% in the control group). Other crustacean peritrophins have shown similar bacterial clearance effects. For example, co-incubation of the recombinant EsPT protein with *V. parahaemolyticus* significantly enhanced bacterial clearance *in vivo* (Huang et al., 2015). In contrast, disruption of EsPT1 impeded the clearance of *V. parahaemolyticus* and led to an increase in the bacterial load (Huang et al., 2015). Similarly, MjCBP in *M. japonicus* demonstrated the ability to promote *V. anguillarum* clearance *in vivo*, whereas knockdown of MjCBP resulted in decreased bacterial clearance (Xu et al., 2021).

To better understand the molecular mechanisms underlying the anti-infective effects of SpPT1, we analyzed the expression of immune-related genes and the activities of several immune-related enzymes after rSpPT1 treatment. We found that the expression of several AMPs, including crustins (SpCrustin3, SpCrustin4, SpCrustin6, and SpCrustin7) and SpALF7, and IMD signaling pathway-related genes SpIMD, SpTAK1, SpIKKε, SpIKKβ, and SpRelish, were significantly upregulated in the hepatopancreas of the rSpPT1-treated group compared to that in the control group. In addition, rSpPT1 treatment significantly increased the

enzymatic activity of acid phosphatase (ACP) and peroxidase (POD) in the hepatopancreas of mud crabs. These results indicate a regulatory role of rSpPT1 in the innate immunity of mud crab. To date, fewer studies have been conducted on the role of peritrophins in immunomodulation, and coupled with the complexity of their specific regulatory mechanisms, futher in-depth investigations should be performed.

5. Conclusions

In summary, the present study identified a new peritrophin homolog (named SpPT1) from the mud crab *S. paramamosain*, which contains a typical ChtBD2. During development, this gene was significantly upregulated in the post-molt stage in juvenile crabs and tissues of subadult crabs, especially in the presence of bacterial exposure. We also found that this gene was modulated by 20E, a key regulator during molting, indicating its role in molting. In adult crabs, SpPT1 gene expression was highest in the midgut, and this gene responded significantly to bacterial challenge in the hepatopancreas. We further obtained the recombinant protein rSpPT1 and investigated its immune related functions. rSpPT1 had no antibacterial activity *in vitro*, but could significantly reduce bacterial load in the hepatopancreas and gills of crabs, and improve the survival rate of crabs infected with *V. alginolyticus*. In addition, rSpPT1 had a strong binding ability to chitin, six common aquatic pathogens and four PAMPs. It was also found that rSpPT1 could promote the phagocytosis of hemocytes. In addition, genes from Toll and IMD signaling pathways and several AMPs, were significantly upregulated after rSpPT1 treatment, as well as the enzymatic activities of ACP and POD, indicating the immune regulatory role of SpPT1. Taken together, the role of the SpPT1 gene revealed in this study will enrich the functional study of the peritrophin family in crabs, and provide a valuable reference for the development of preventive and therapeutic strategies for molt failure caused by pathogens in crab farms.

CRediT authorship contribution statement

Roushi Chen: Writing – original draft, Methodology, Investigation, Formal analysis, Data curation. **Jiaojiao Yan:** Methodology, Investigation, Formal analysis. **Shuang Li:** Methodology, Investigation, Formal analysis. **Ke-Jian Wang:** Writing – review & editing, Project administration, Funding acquisition. **Fangyi Chen:** Writing – review & editing, Supervision, Project administration, Funding acquisition, Conceptualization.

Declaration of competing interest

The authors declare that the research was conducted in the absence of any commercial or financial relationships that could be construed as a potential conflict of interest.

Data availability

No data was used for the research described in the article.

Acknowledgments

This study was supported by grant U1805233/42376089/41806162 from the National Natural Science Foundation of China; grant 2021J05008 from the Natural Science Foundation of Fujian Province, China; grant FJHY-YYKJ-2024-2-3 and FJHY-YYKJ-2022-1-14 from Fujian Ocean and Fisheries Bureau; grant FOCAL2023-0207 from Fujian Ocean Synergy Alliance (FOCAL) and grant 22CZP002HJ08 from Xiamen Ocean Development Bureau, and grant Z20220743 from Pingtan Research Institute of Xiamen University. We thank laboratory engineers Hui Peng, Huiyun Chen, Zhiyong Lin, Hua Hao and Ming Xiong for providing technical assistance.

References

Abedi, Z., Brown, A., 1961. Peritrophic membrane as vehicle for DDT and DDE excretion in *Aedes aegypti* larvae. Ann. Entomol. Soc. Am. 54 (4), 539–542.
Barbehenn, R.V., Martin, M.M., 1992. The protective role of the peritrophic membrane in the tannin-tolerant larvae of *Orgyia leucostigma* (Lepidoptera). J. Insect Physiol. 38 (12), 973–980.
Chen, F., Wang, K., 2019. Characterization of the innate immunity in the mud crab *Scylla paramamosain*. Fish Shellfish Immunol. 93, 436–448.
Chen, W.J., Huang, L.X., Hu, D., Liu, L.Y., Gu, J., Huang, L.H., Feng, Q.L., 2014. Cloning, expression and chitin-binding activity of two peritrophin-like protein genes in the common cutworm, *Spodoptera litura*. Insect Sci. 21 (4), 449–458.
Chen, Y.L., Kumar, R., Liu, C.H., Wang, H.C., 2022. *Litopenaeus vannamei* peritrophin interacts with WSSV and AHPND-causing *V. Parahaemolyticus* to regulate disease pathogenesis. Fish Shellfish Immunol. 126, 271–282.
Devenport, M., Alvarenga, P.H., Shao, L., Fujioka, H., Bianconi, M.L., Oliveira, P.L., Jacobs-Lorena, M., 2006. Identification of the *Aedes aegypti* peritrophic matrix protein AeIMUCI as a heme-binding protein. Biochemistry 45 (31), 9540–9549.
Dong, X., Wang, X., Chen, X., Yan, Z., Cheng, J., Gao, L., Liu, Y., Li, J., 2017. Genetic diversity and virulence potential of *Staphylococcus aureus* isolated from crayfish (*Procambarus clarkii*). Curr. Microbiol. 74, 28–33.
Du, X.J., Wang, J.X., Liu, N., Zhao, X.F., Li, F.H., Xiang, J.H., 2006. Identification and molecular characterization of a peritrophin-like protein from fleshy prawn (*Fenneropenaeus chinensis*). Mol. Immunol. 43 (10), 1633–1644.
Eisemann, C.H., Binnington, K.C., 1994. The peritrophic membrane: its formation, structure, chemical composition and permeability in relation to vaccination against ectoparasitic arthropods. Int. J. Parasitol. 24 (1), 15–26.
Espinoza-Fuentes, F., Terra, W.R., 1987. Physiological adaptations for digesting bacteria. Water fluxes and distribution of digestive enzymes in *Musca domestica* larval midgut. Insect Biochemistry. 17 (6), 809–817.
Gong, J., Yu, K., Shu, L., Ye, H., Li, S., Zeng, C., 2015. Evaluating the effects of temperature, salinity, starvation and autotomy on molting success, molting interval and expression of ecdysone receptor in early juvenile mud crabs, *Scylla paramamosain*. J. Exp. Mar. Biol. Ecol. 464, 11–17.
Han, F., Wang, X., Guo, J., Qi, C., Xu, C., Luo, Y., Li, E., Qin, J.G., Chen, L., 2019. Effects of glycinin and β-conglycinin on growth performance and intestinal health in juvenile Chinese mitten crabs (*Eriocheir sinensis*). Fish Shellfish Immunol. 84, 269–279.
Hegedus, D.D., Toprak, U., Erlandson, M., 2019. Peritrophic matrix formation. J. Insect Physiol. 117, 103898.
Huang, Y., Ma, F., Wang, W., Ren, Q., 2015. Identification and molecular characterization of a peritrophin-like gene, involved in the antibacterial response in Chinese mitten crab, *Eriocheir sinensis*. Dev Comp Immunol. 50 (2), 129–138.
Jasrapuria, S., Arakane, Y., Osman, G., Kramer, K.J., Beeman, R.W., Muthukrishnan, S., 2010. Genes encoding proteins with peritrophin A-type chitin-binding domains in *Tribolium castaneum* are grouped into three distinct families based on phylogeny, expression and function. Insect Biochem. Mol. Biol. 40 (3), 214–227.
Jasrapuria, S., Specht, C.A., Kramer, K.J., Beeman, R.W., Muthukrishnan, S., 2012. Gene families of cuticular proteins analogous to peritrophins (CPAPs) in *Tribolium castaneum* have diverse functions. PloS One 7 (11), e49844.
Jiang, M., Chen, R., Chen, F., Zhu, X., Wang, K.J., 2022. A new crustin gene homolog SpCrus8 identified in *Scylla paramamosain* exerting *in vivo* protection through opsonization and immunomodulation. Front. Immunol. 13, 946227.
Khayat, M., Babin, P.J., Funkenstein, B., Sammar, M., Nagasawa, H., Tietz, A., Lubzens, E., 2001. Molecular characterization and high expression during oocyte development of a shrimp ovarian cortical rod protein homologous to insect intestinal peritrophins. Biol. Reprod. 64 (4), 1090–1099.
Konno, K., Mitsuhashi, W., 2019. The peritrophic membrane as a target of proteins that play important roles in plant defense and microbial attack. J. Insect Physiol. 117, 103912.
Kun, Q., Ya-Qun, Z., Shu-Ping, W., Zhe, A.N., Hua, H., Fang-Yi, C., Hui, P., 2014. The optimization of primary hemocyte culture of *Scylla paramamosain*. China Animal Husbandry & Veterinary Medicine. 41 (09), 145–149.
Kuraishi, T., Binggeli, O., Opota, O., Buchon, N., Lemaitre, B., 2011. Genetic evidence for a protective role of the peritrophic matrix against intestinal bacterial infection in *Drosophila melanogaster*. Proc. Natl. Acad. Sci. U. S. A. 108 (38), 15966–15971.
Li, J., Qiu, W., Hao, H., Chen, F., Wang, K.J., 2022. Morphology of the complete embryonic and larval development of commercially important mud crab *Scylla paramamosain*. Aquacult. Res. 53 (6), 2298–2316.
Li, S., Li, W., Chen, F., Zhu, X., Chen, H.-Y., Hao, H., Wang, K.-J., 2023. Metabolomic and transcriptomic analysis reveals immune and hormone modulation at the molting stage of juvenile mud crabs challenged with *Staphylococcus aureus* and *Vibrio alginolyticus*. Aquaculture 575, 739775.
Liu, X., Zhang, J., Zhu, K.Y., 2019. Chitin in arthropods: biosynthesis, modification, and metabolism. Adv. Exp. Med. Biol. 1142, 169–207.
Livak, K.J., Schmittgen, T.D., 2001. Analysis of relative gene expression data using real-time quantitative PCR and the 2(-Delta Delta C(T)) method. Methods 25 (4), 402–408.
Loongyai, W., Avarre, J.C., Cerutti, M., Lubzens, E., Chotigeat, W., 2007. Isolation and functional characterization of a new shrimp ovarian peritrophin with antimicrobial activity from *Fenneropenaeus merguiensis*. Mar. Biotechnol. (N.Y.) 9 (5), 624–637.
Lu, Y., Su, F., Li, Q., Zhang, J., Li, Y., Tang, T., Hu, Q., Yu, X.Q., 2020. Pattern recognition receptors in Drosophila immune responses. Dev. Comp. Immunol. 102, 103468.
Ma, H., Chu, J., Wang, L., Li, F., Xiang, J., 2017. Cloning and expression analysis of shrimp ovarian peritrophin-like gene during early embryonic development in *Litopenaeus vannamei*. J. Fish. China 41 (5), 649–657.

Merzendorfer, H., 2013. Insect-derived chitinases. Adv. Biochem. Eng. Biotechnol. 136, 19–50.
Peters, W., 2012. Peritrophic Membranes. Springer Science & Business Media.
Qiu, W., Chen, F., Chen, R., Li, S., Zhu, X., Xiong, M., Wang, K.J., 2021. A new C-type lectin homolog SpCTL6 exerting immunoprotective effect and regulatory role in mud crab *Scylla paramamosain*. Front. Immunol. 12, 661823.
Richards, A.G., Richards, P.A., 1977. The peritrophic membranes of insects. Annu. Rev. Entomol. 22, 219–240.
Rodríguez-de la Noval, C., Rodríguez-Cabrera, L., Izquierdo, L., Espinosa, L.A., Hernandez, D., Ponce, M., Moran-Bertot, I., Tellez-Rodríguez, P., Borras-Hidalgo, O., Huang, S., Kan, Y., Wright, D.J., Ayra-Pardo, C., 2019. Functional expression of a peritrophin A-like SfPER protein is required for larval development in *Spodoptera frugiperda* (Lepidoptera: Noctuidae). Sci. Rep. 9 (1), 2630.
Sandoval-Mojica, A.F., Scharf, M.E., 2016. Gut genes associated with the peritrophic matrix in *Reticulitermes flavipes* (Blattodea: Rhinotermitidae): identification and characterization. Arch. Insect Biochem. Physiol. 92 (2), 127–142.
Tellam, R., Vuocolo, T., Eisemann, C., Briscoe, S., Riding, G., Elvin, C., Pearson, R., 2003. Identification of an immuno-protective mucin-like protein, peritrophin-55, from the peritrophic matrix of *Lucilia cuprina* larvae. Insect Biochem. Mol. Biol. 33 (2), 239–252.
Tellam, R.L., Wijffels, G., Willadsen, P., 1999. Peritrophic matrix proteins. Insect Biochem. Mol. Biol. 29 (2), 87–101.
Tellam, R.L., Eisemann, C., Casu, R., Pearson, R., 2000. The intrinsic peritrophic matrix protein peritrophin-95 from larvae of *Lucilia cuprina* is synthesised in the cardia and regurgitated or excreted as a highly immunogenic protein. Insect Biochem. Mol. Biol. 30 (1), 9–17.
Thuong, K.V., Tuan, V.V., Li, W., Sorgeloos, P., Bossier, P., Nauwynck, H., 2016. Per os infectivity of white spot syndrome virus (WSSV) in white-legged shrimp (*Litopenaeus vannamei*) and role of peritrophic membrane. Vet. Res. 47, 39.
Tynyakov, J., Bentov, S., Abehsera, S., Khalaila, I., Manor, R., Katzir Abilevich, L., Weil, S., Aflalo, E.D., Sagi, A., 2015. A novel chitin binding crayfish molar tooth protein with elasticity properties. PloS One 10 (5), e0127871.
Vuocolo, T., Eisemann, C.H., Pearson, R.D., Willadsen, P., Tellam, R.L., 2001. Identification and molecular characterisation of a peritrophin gene, peritrophin-48, from the myiasis fly *Chrysomya bezziana*. Insect Biochem. Mol. Biol. 31 (9), 919–932.
Wang, D., Wu, F., 2023. China Fisheries Statistical Yearbook. China Agriculture Press.
Wang, L., Li, F., Wang, B., Xiang, J., 2013. A new shrimp peritrophin-like gene from *Exopalaemon carinicauda* involved in white spot syndrome virus (WSSV) infection. Fish Shellfish Immunol. 35 (3), 840–846.
Wang, P., Granados, R.R., 1997. Molecular cloning and sequencing of a novel invertebrate intestinal mucin cDNA. J. Biol. Chem. 272 (26), 16663–16669.
Wang, P., Granados, R.R., 2001. Molecular structure of the peritrophic membrane (PM): identification of potential PM target sites for insect control. Arch. Insect Biochem. Physiol. 47 (2), 110–118.
Wang, Y., Cheng, J., Luo, M., Wu, J., Guo, G., 2020. Identifying and characterizing a novel peritrophic matrix protein (MdPM-17) associated with antibacterial response from the housefly, *Musca domestica* (Diptera: Muscidae). J. Insect Sci. 20 (6).
Wu, K., Yang, B., Huang, W., Dobens, L., Song, H., Ling, E., 2016. Gut immunity in lepidopteran insects. Dev. Comp. Immunol. 64, 65–74.
Xie, S., Zhang, X., Zhang, J., Li, F., Xiang, J., 2015. Envelope proteins of white spot syndrome virus (WSSV) interact with *Litopenaeus vannamei* peritrophin-like orotein (LvPT). PloS One 10 (12), e0144922.
Xu, S., Jing, M., Kong, D.M., Wang, Y.R., Zhou, Q., Liu, W.Y., Jiao, F., Li, Y.J., Xie, S.Y., 2021. Chitin binding protein from the kuruma shrimp *Marsupenaeus japonicus* facilitates the clearance of *Vibrio anguillarum*. Dev. Comp. Immunol. 117, 103981.
Xu, Z., Liu, A., Li, S., Wang, G., Ye, H., 2020. Hepatopancreas immune response during molt cycle in the mud crab, *Scylla paramamosain*. Sci Rep. 10 (1), 13102.
Yan, T., 2012. Several causes of molt failure in *Scylla serrata* and methods of prevention and control. Fishery Guide to be Rich. 8, 44–45.
Yang, Y., Chen, F., Chen, H.-Y., Peng, H., Hao, H., Wang, K.-J., 2020. A novel antimicrobial peptide scyreprocin from mud crab *Scylla paramamosain* showing potent antifungal and anti-biofilm activity. Front. Microbiol. 11, 1589.
Zha, X.L., Yu, X.B., Zhang, H.Y., Wang, H., Huang, X.Z., Shen, Y.H., Lu, C., 2020. Identification of peritrophins and antiviral effect of Bm01504 against BmNPV in the silkworm, *Bombyx mori*. Int J Mol Sci. 21 (21).
Zhou, J., Zhou, J.F., Wang, Y., Feng, G.P., Fang, W.H., Kang, W., Ma, L.B., Li, X.C., 2021. SpSR-B2 functions as a potential pattern recognition receptor involved in antiviral and antibacterial immune responses of mud crab *Scylla paramamosain*. Int. J. Biol. Macromol. 193, 2173–2182.
Zhu, D., Chen, F., Chen, Y.C., Peng, H., Wang, K.J., 2021. The long-term effect of a nine amino-acid antimicrobial peptide AS-hepc3((48-56)) against *Pseudomonas aeruginosa* with no detectable resistance. Front. Cell. Infect. Microbiol. 11, 752637.